

# High-power, single-frequency, continuous-wave second-harmonic-generation of ytterbium fiber laser in PPKTP and MgO:sPPLT

S. Chaitanya Kumar,<sup>1,\*</sup> G. K. Samanta,<sup>1</sup> and M. Ebrahim-Zadeh<sup>1,2</sup>

<sup>1</sup>ICFO-Institut de Ciències Fotoniques, Mediterranean Technology Park, 08860 Castelldefels, Barcelona, Spain

<sup>2</sup>Institució Catalana de Recerca i Estudis Avançats (ICREA), Passeig Lluís Companys 23, Barcelona 08010, Spain

\*[chaitanya.suddapalli@icfo.es](mailto:chaitanya.suddapalli@icfo.es)

**Abstract:** Characteristics of high-power, narrow-linewidth, continuous-wave (cw) green radiation obtained by simple single-pass second-harmonic-generation (SHG) of a cw ytterbium fiber laser at 1064 nm in the nonlinear crystals of PPKTP and MgO:sPPLT are studied and compared. Temperature tuning and SHG power scaling up to nearly 10 W for input fundamental power levels up to 30 W are performed. Various contributions to thermal effects in both crystals, limiting the SHG conversion efficiency, are studied. Optimal focusing conditions and thermal management schemes are investigated to maximize SHG performance in MgO:sPPLT. Stable green output power and high spatial beam quality with  $M^2 < 1.33$  and  $M^2 < 1.34$  is achieved in MgO:sPPLT and PPKTP, respectively.

©2009 Optical Society of America

**OCIS codes:** (190.2620) Harmonic generation and mixing; (190.4400) Nonlinear optics, materials; (140.3510) Lasers, fiber; (140.7300) Visible lasers.

---

## References and links

1. J. Golden, "Green lasers score good marks in semiconductor material processing," *Laser Focus World*, **28**, 75 (1992).
2. R. J. Rockwell, Jr., M.S., "Designs and functions of laser systems for biomedical applications", in Conference on the laser, *Annals of the New York Academy of Sciences*, **168**, 2 (2006).
3. K. Yamamoto, H. Furuya, and K. Mizuuchi, "Highly-efficient SHG laser by using periodically poled MgO:LiNbO<sub>3</sub> and its application," in proceedings of Lasers and Electro-Optics Society, **693** (IEEE, 2007), paper ThA3.
4. G. K. Samanta, S. Chaitanya Kumar, R. Das, and M. Ebrahim-Zadeh, "Continuous-wave optical parametric oscillator pumped by a fiber laser green source at 532 nm," *Opt. Lett.* **34**, 2255-2257 (2009).
5. R. G. Batchko, G. D. Miller, A. Alexandrovski, M. M. Fejer, and R. L. Byer, In Proceedings of the Conference on Lasers and Electro-Optics, (Optical Society of America, Washington, D.C., 1998), **12**, 75 (1998).
6. J. D. Bierlein and H. Vanherzele, "Potassium titanyl phosphate: properties and new applications," *J. Opt. Soc. Am. B* **6**, 622-633 (1989).
7. Z. Sun, G. K. Samanta, G. R. Fayaz, M. Ebrahim-Zadeh, C. Canalias, V. Pasiskevicius, and F. Laurell, "Efficient generation of tunable CW single frequency green radiation by second harmonic generation in periodically-poled KTiOPO<sub>4</sub>," in Proceedings of the Conference on Lasers and Electro-Optics (Optical Society of America, 2007), paper CTuK1.
8. G. K. Samanta, S. Chaitanya Kumar, M. Mathew, C. Canalias, V. Pasiskevicius, F. Laurell, and M. Ebrahim-Zadeh, "High-power, continuous-wave, second-harmonic generation at 532 nm in periodically poled KTiOPO<sub>4</sub>," *Opt. Lett.* **33**, 2955-2957 (2008).
9. N. E. Yu, S. Kurimura, Y. Nomura, and K. Kitamura, "Stable high-power green light generation with thermally conductive periodically poled stoichiometric lithium tantalate," *Jpn. J. Appl. Phys.* **43**, L1265 – L1267 (2004).
10. S. V. Tovstonog, S. Kurimura, I. Suzuki, K. Takeno, S. Moriwaki, N. Ohmae, N. Mio, and T. Katagai, "Thermal effects in high-power CW second harmonic generation in Mg-doped stoichiometric lithium tantalate," *Opt. Express* **16**, 11294-11299 (2008).
11. G. K. Samanta, S. Chaitanya Kumar, and M. Ebrahim-Zadeh, "Stable, 9.6 W, continuous-wave, single-frequency, fiber-based green source at 532 nm," *Opt. Lett.* **34**, 1561-1563 (2009).

12. D. S. Hum, R. K. Route, G. D. Miller, V. Kondilenko, A. Alexandrovski, J. Huang, K. Urbanek, R. L. Byer, and M. M. Fejer, "Optical properties and ferroelectric engineering of vapor-transport-equilibrated, near-stoichiometric lithium tantalate for frequency conversion," *J. Appl. Phys.* **101**, 093108 (2007).
13. The PPKTP crystal was fabricated by C. Canalias, V. Pasiskevicius, and F. Laurell, Royal Institute of Technology, Sweden.
14. The MgO:sPPLT crystal was fabricated by HC Photonics Corporation, Taiwan.
15. K. Kato and E. Takaoka, "Sellmeier and thermo-optic dispersion formulas for KTP," *Appl. Opt.* **41**, 5040-5044 (2002).
16. A. Bruner, D. Eger, M. B. Oron, P. Blau, M. Katz, and S. Ruschin, "Temperature-dependent Sellmeier equation for the refractive index of stoichiometric lithium tantalite," *Opt. Lett.* **28**, 194-196 (2003).
17. M. M. Fejer, G. A. Magel, D. H. Jundt, and R. L. Byer, "Quasi-phase-matched second harmonic generation: Tuning and tolerances," *IEEE J. Quantum Elect.* **28**, 2631-2654 (1992).
18. G. D. Boyd and D. A. Kleinman, "Parametric interaction of focused Gaussian light beams," *J. Appl. Phys.* **39**, 3597-3639 (1968).
19. K. Kitamura, Y. Furukawa, S. Takekawa, T. Hatanaka, H. Ito, and V. Gopalan, "Non-stoichiometric control of LiNbO<sub>3</sub> and LiTaO<sub>3</sub> in ferroelectric domain engineering for optical devices," *Ferroelectrics* **257**, 235 - 243 (2001)
20. G. K. Samanta, and M. Ebrahim-Zadeh, "Continuous-wave singly-resonant optical parametric oscillator with resonant wave coupling," *Opt. Express* **16**, 6883-6888 (2008).
21. Z. M. Liao, S. A. Payne, J. Dawson, A. Droboschoff, C. Ebberts, D. Pennington, and L. Taylor, "Thermally induced dephasing in periodically poled KTP frequency-doubling crystals," *J. Opt. Soc. Am. B* **21**, 2191-2196 (2004).
22. H. Hatano, S. Takekawa, S. Kurimura, O. A. Louchev, and K. Kitamura, "Thermal managements for highly efficient SHG with linear input/output characteristics using periodically poled stoichiometric LiTaO<sub>3</sub>," in *Proceedings of the Conference on Lasers and Electro-Optics (Optical Society of America, 2007)*, paper CMBB5.

## 1. Introduction

Compact, high-power, green lasers are of interest for a variety of scientific and technological applications such as material processing [1], human surgery [2], and laser display technology [3]. In continuous-wave (cw), single-frequency operation, they hold promise as pumps for singly-resonant optical parametric oscillators (SROs) [4] and Ti:sapphire lasers. The combination of a cw infrared fiber laser and a simple single-pass second-harmonic-generation (SHG) scheme based on periodically poled nonlinear crystals is a potentially attractive approach for high-power cw green generation, not only because of its compact and practical architecture, but also due to the narrow linewidth and high spatial beam quality that are inherently transferable from the fiber pump laser to the green output. With the rapid advances in fiber laser technology, access to high cw fundamental powers of tens of watts is also no longer a limitation, making the choice of nonlinear material the most critical factor in the attainment of high optical powers and practical single-pass SHG efficiencies. In this regard, the most important material properties include high optical nonlinearity, long interaction length, noncritical phase-matching capability, and high optical damage threshold to withstand the large cw optical intensities. These requirements can be met by the new generation of quasi-phase-matched (QPM) nonlinear crystals. Although the well-established nonlinear material, periodically poled LiNbO<sub>3</sub> (PPLN), with high effective nonlinearity ( $d_{eff} \sim 16$  pm/V), can in principle enable SHG into the visible spectral range, in practice stable and room-temperature operation is problematic due to the photorefractive effect, with increasing difficulty at higher power levels. Doping PPLN with MgO (MgO:PPLN) not only reduces the photorefractive effect, but also increases the laser damage threshold. However, SHG into the green using MgO:PPLN is still limited by green-induced infrared absorption (GRIIRA) effects [5]. Periodically poled KTiOPO<sub>4</sub> (PPKTP), with relatively high effective nonlinearity ( $d_{eff} \sim 10$  pm/V) and high damage threshold [6], is another interesting nonlinear material for SHG into the green. With its low susceptibility to photorefractive damage, PPKTP can permit the generation of several watts of frequency-doubled green light at room temperature. However, the high sensitivity of PPKTP to defect-induced absorption, the so-called gray tracking, and other optically-induced thermal effects resulting from absorption of the fundamental and generated second harmonic green light, have been the major limiting factors in improving output power and beam quality. Despite these thermal effects, PPKTP has so far been

effectively used for cw green light generation in various configurations. Earlier reports include single-pass SHG of a Yb:YAG thin-disk solid-state laser in PPKTP, providing 1.2 W of cw single-frequency green radiation for 13.6 W of fundamental power at a conversion efficiency of 8.8% [7]. Only recently, we reported a fiber-laser-based SHG device providing 6.2 W of cw single-frequency green output at a single-pass conversion efficiency of 20.8% [8]. At the same time, the emergence of other QPM nonlinear materials such as MgO-doped periodically poled stoichiometric LiTaO<sub>3</sub> (MgO:sPPLT) with improved optical and thermal properties [9], along with increased resistance to photorefractive damage and GRIIRA, has provided an attractive new alternative to further overcome the limitations due to thermal effects to permit cw green radiation at elevated power levels. Earlier reports include external single-pass SHG of a 91.5-W Nd:YAG laser in MgO:sPPLT, providing a maximum single-mode green power of 16.1 W at 532 nm at a conversion efficiency of 17.6% [10]. Most recently, we also reported the generation of 9.6 W of green radiation at 532 nm using single-pass SHG of a ytterbium fiber laser in MgO:sPPLT at 32.7% conversion efficiency [11]. Saturation of SHG efficiency and power has been observed in both PPKTP and MgO:sPPLT at high input fundamental powers due to thermal phase-mismatch effects [8,10], indicating that achieving high output power and at the same time retaining single-frequency operation along with good spatial beam quality are important challenges to overcome. Although it is pointed out that light-induced absorption at the fundamental [12] and second harmonic [10] wavelengths cause crystal heating, the true origin of thermal effects is still not completely clear. Hence, a comprehensive study of high-power SHG in both PPKTP and MgO:sPPLT is of considerable importance.

In the present work, we perform a detailed study and compare the characteristics of PPKTP and MgO:sPPLT crystals for high-power cw SHG in external single-pass configuration using a 30-W cw, single-frequency ytterbium fiber laser at 1064 nm. Temperature tuning properties of the two crystals are compared at different fundamental power levels up to a maximum available 30 W. Measurements at low input power of ~1 W are used to estimate the temperature acceptance bandwidth and effective nonlinearity of the crystals. Power scaling of SHG has been performed to characterize the crystals for maximum attainable green output, and power stability measurements are compared to gain insight into thermal effects that set in at high input fundamental powers. Optimal focusing conditions and thermal management schemes have been investigated to maximize output power and SHG conversion efficiency. Single-frequency performance and frequency stability characteristics of the generated green radiation are studied, and spatial beam quality measurements of the output are presented.

## 2. Experimental setup

The schematic of experimental setup for single-pass SHG experiments is shown in Fig. 1. The fundamental pump source is a cw ytterbium fiber laser (IPG Photonics, YLR-30-1064-LP-SF) delivering linearly polarized single-frequency radiation at 1064 nm with a maximum output power of 30 W with a power stability of <1% over one hour and a nominal linewidth of 89 kHz. Using a confocal scanning Fabry-Perot interferometer (free-spectral-range ~ 1 GHz, finesse ~ 400), we confirm single-frequency operation of the laser, with a measured linewidth of 12.5 MHz, limited by the resolution of the interferometer. The frequency stability of the fiber laser is measured to be <120 MHz over one hour and <50 MHz over 30 minutes [4], while the power stability is measured to be <1% over 65 minutes. An isolator at the output end of the fiber protects the laser from any back-reflections. Using a 25 cm focal length lens and a scanning beam profiler, we measured the laser to have a beam quality factor  $M^2 < 1.01$ . In order to maintain stable output characteristics, the pump laser is operated at maximum power and the input power to the SHG crystal is adjusted by using a combination of half-wave plate and polarizing beam-splitter cube. A second half-wave plate is used to obtain the correct polarization for phase-matched SHG in the nonlinear crystal. The fundamental beam is focused into the SHG crystal using a single lens, with the resulting beam waist positioned at the center of the crystal. The nonlinear crystals used in the experiments are bulk PPKTP [13]

and MgO:sPPLT [14]. The PPKTP crystal was 19-mm-long, 1-mm-thick, and 6-mm-wide flux-grown KTP sample containing a single grating period of 9.01  $\mu\text{m}$ . The actual length of the grating over the sample was 17 mm.

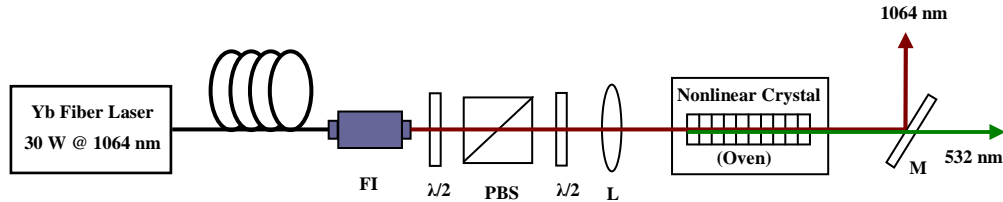


Fig. 1. Experimental setup for single-pass second harmonic generation. FI: Faraday isolator,  $\lambda/2$ : Half-wave plate, PBS: Polarizing beam-splitter, L: Lens, M: Dichroic mirror.

The MgO:sPPLT crystal was 30-mm-long, 1-mm-thick, 2.14-mm-wide, with a single grating period of 7.97  $\mu\text{m}$ . The end faces of both the crystals were antireflection-coated ( $R < 1\%$ ) at 1064 nm and 532 nm. Each crystal was directly mounted in an oven with a temperature stability of better than  $\pm 0.1$   $^{\circ}\text{C}$ . No interface material such as thermal paste or copper foil was used for heat exchange between the crystal and oven. A dichroic mirror, M, coated for high reflectivity ( $R > 99\%$ ) at 1064 nm and high transmission ( $T > 94\%$ ) at 532 nm, was used to extract the generated green output from the fundamental.

In order to achieve efficient SHG, we first studied temperature phase-matching properties of the two crystals, evaluating the acceptance bandwidth, phase-matching temperature, and rate of change of phase-matching temperature with fundamental power.

### 3. Temperature tuning

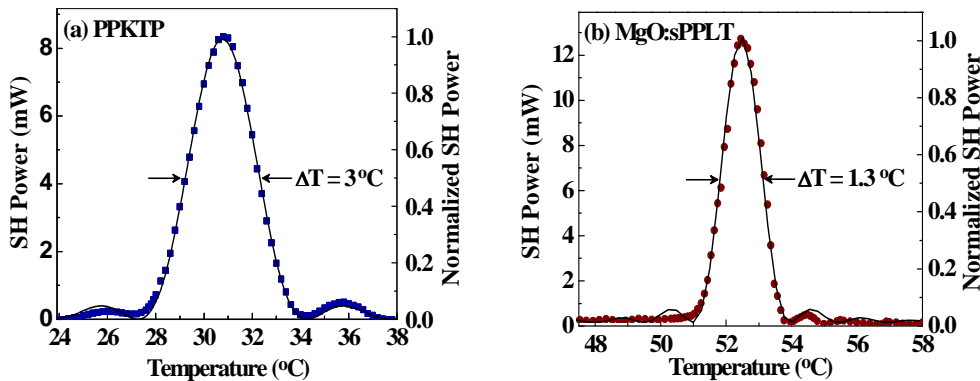


Fig. 2. Temperature tuning curves of (a) PPKTP and (b) MgO:sPPLT, at approximately 1 W of incident fundamental power.

The variation of the second harmonic output with temperature at a fixed fundamental wavelength determines the temperature acceptance bandwidth of the nonlinear crystal and provides information about the uniformity of phase-matching throughout the crystal length. The SHG temperature tuning curves obtained for PPKTP and MgO:sPPLT crystals are shown in the Fig. 2. The measurements were performed using a fundamental beam waist radius 37  $\mu\text{m}$  corresponding to a focusing parameter of  $\xi = 1.74$  in case of MgO:sPPLT and  $\xi = 1.28$  in case of PPKTP at a fundamental power of approximately 1 W, in order to avoid any unwanted contributions from thermal effects. The  $\text{sinc}^2$  fit to the experimental data has a full-width at half-maximum (FWHM) bandwidth of  $\Delta T = 3$   $^{\circ}\text{C}$  at a phase-matching temperature of 30.8  $^{\circ}\text{C}$  for PPKTP, and  $\Delta T = 1.3$   $^{\circ}\text{C}$  at a phase-matching temperature of 52.5  $^{\circ}\text{C}$  for MgO:sPPLT. These values are slightly wider than the calculated values of 2.62  $^{\circ}\text{C}$  and 0.96  $^{\circ}\text{C}$ , respectively, using the relevant Sellmeier equations [15,16]. The temperature acceptance bandwidth is calculated using the relation [17],

$$\Delta T = \frac{0.4429\lambda_{\omega}}{L} \left[ \frac{\partial n_{2\omega}}{\partial T} - \frac{\partial n_{\omega}}{\partial T} - \alpha(n_{2\omega} - n_{\omega}) \right]^{-1}, \quad (1)$$

where  $\Delta T$  is the FWHM of the temperature tuning curve,  $L$  is the crystal length,  $\lambda_{\omega}$  is the fundamental wavelength,  $n_{\omega}$  and  $n_{2\omega}$  are the refractive indices at the fundamental and second harmonic wavelengths, and  $\alpha$  is the linear thermal expansion coefficient of the crystal. The derivatives are evaluated at the respective phase-matching temperatures. The discrepancy between the calculated and measured temperature acceptance bandwidth values arises from various factors including focusing, non-uniformity of the grating period and thermal effects. As the measurements were performed at low fundamental power, avoiding any contribution from thermal effects, the mismatch in the calculated and measured temperature acceptance bandwidth values can be possibly associated with focusing and non-uniformity of the grating period along the length of the crystal. The close agreement between the measured temperature tuning data and the ideal sinc<sup>2</sup> functions in Fig. 2 implies good homogeneity of refractive index at lower input power levels, resulting in a symmetric phase-matching curve. The wide temperature acceptance bandwidth measured for PPKTP in comparison with that of MgO:sPPLT, which is due to the shorter interaction length, indicates

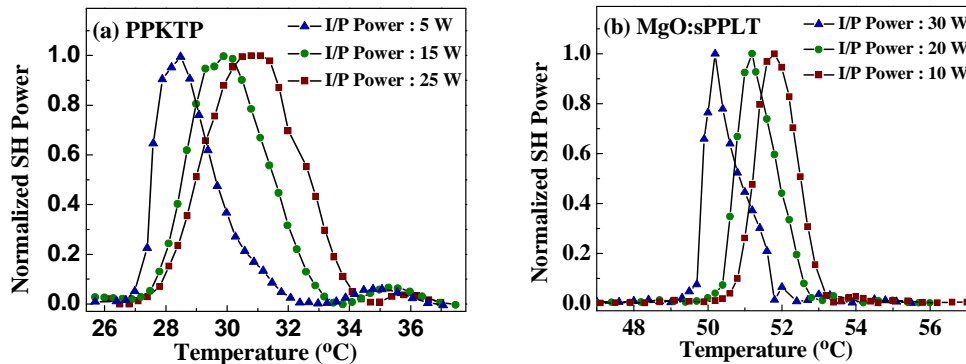


Fig. 3. Temperature tuning curves of (a) PPKTP and (b) MgO:sPPLT at different fundamental power levels.

that the generated SH power is less susceptible to minor temperature fluctuations. However, at higher incident fundamental powers, material absorption is expected to become increasingly important, leading to heating of the nonlinear crystal. As a result, the oven temperature has to be lowered to compensate for the rise in crystal temperature, thus resulting in a shift of the phase-matching peak towards lower temperatures. This is confirmed by measurements and the results are shown in Fig. 3. This shift is stronger in PPKTP than in MgO:sPPLT, which can be attributed to the higher thermal conductivity of the MgO:sPPLT crystal [9]. Also, the sinc<sup>2</sup> phase-matching curve loses its typical symmetric shape at higher input powers, which can be attributed to thermal dephasing due to inhomogeneous temperature distribution in the nonlinear crystal arising from light-induced absorption at higher fundamental powers. It can also be seen from Fig. 3 that the temperature acceptance bandwidth shrinks to lower values with increasing input power. We attribute this to increased thermal dephasing over the interaction length of the crystal at higher input fundamental powers. The phase-matching temperature decreases with the fundamental power ( $P_{\omega}$ ) at a rate of 0.14 °C/W for PPKTP and 0.08 °C/W for MgO:sPPLT, as shown in Fig. 4, indicating that MgO:sPPLT is more resistant to light-induced thermal effects than PPKTP. It is also to be noted that the spectral acceptance bandwidths of the two nonlinear crystals, calculated from the Sellmeier equations [15,16], are 0.157 nm (41.7 GHz) and 0.082 nm (21.8 GHz) for PPKTP and MgO:sPPLT, respectively.

These values are substantially larger than the fundamental linewidth of 89 kHz, confirming that the fiber laser bandwidth is not a limiting factor in the attainment of efficient SHG.

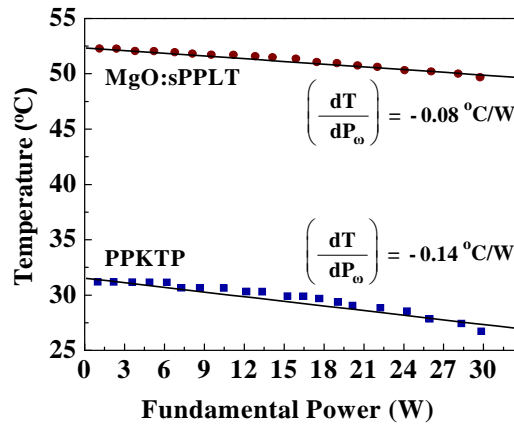


Fig. 4. Dependence of the phase-matching temperature on fundamental power for PPKTP and MgO:sPPLT crystals.

#### 4. Power scaling

The variation of the generated green power with input fundamental power determines the efficiency of the SHG process and also provides information about the artifacts of the light-induced thermal effects on SH power and efficiency. In order to compare the performance of the two crystals, the power scaling measurements were performed under similar focusing conditions. The fundamental beam was focused at the center of the 17-mm-long PPKTP crystal to a beam waist radius of 37  $\mu\text{m}$ , corresponding to a focusing parameter,  $\xi = (L/b) = 1.28$ . Here  $L$  is the crystal length and  $b = kw_{op}^2$  is the confocal parameter, with  $k = 2\pi n_{\omega} / \lambda_{\omega}$ .

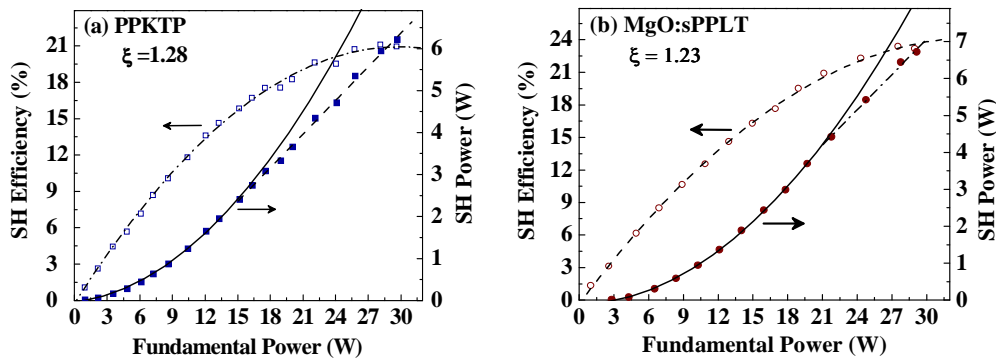


Fig. 5. Dependence of measured SH power and corresponding conversion efficiency on the incident fundamental power for (a) PPKTP, (b) MgO:sPPLT.

where  $n_{\omega}$ ,  $\lambda_{\omega}$ , and  $w_{op}$  are the refractive index, wavelength, and waist radius of the fundamental beam inside the crystal, respectively [18]. A similar focusing parameter of  $\xi = 1.23$  in the 30-mm-long MgO:sPPLT crystal requires the fundamental beam waist radius at the center of the crystal to be 44  $\mu\text{m}$ . The measured SH power and efficiency up to a maximum available fundamental power of 30 W are shown in Fig. 5. The fundamental power was measured at the input to the crystal, while the generated green power was corrected for the 6% transmission loss of the mirror, M (Fig. 1), used to separate the generated SH from the

fundamental. A maximum green power of 6.2 W was obtained at a fundamental power of 29.75 W in PPKTP, corresponding to a single-pass conversion efficiency of 20.8%, while the maximum green power obtained with MgO:sPPLT was 6.7 W at a fundamental power of 28.9 W, corresponding to a single-pass conversion efficiency of 23.1%. From Fig. 5(a) it can be seen that the generated SH power in PPKTP shows the expected quadratic dependence from the low-power regime up to ~16 W of fundamental power, above which it exhibits a linear variation. In MgO:sPPLT, the SH power maintains quadratic dependence up to ~21 W of fundamental power, as evident in Fig. 5(b). Also, in both cases, the SH efficiency begins to saturate at the respective input power levels, which can be attributed to pump depletion and the onset of thermal phase-mismatch effects under this focusing condition. This is further evident from the dependence of SH power on the square of fundamental power, as shown in Fig. 6. The deviation from the linear dependence of SH power on the square of fundamental power is clearly seen in both PPKTP and MgO:sPPLT, but occurs at a higher fundamental power in MgO:sPPLT. In an effort to improve SH power and efficiency, we also attempted other focusing conditions, corresponding to smaller beam waists, in both crystals.

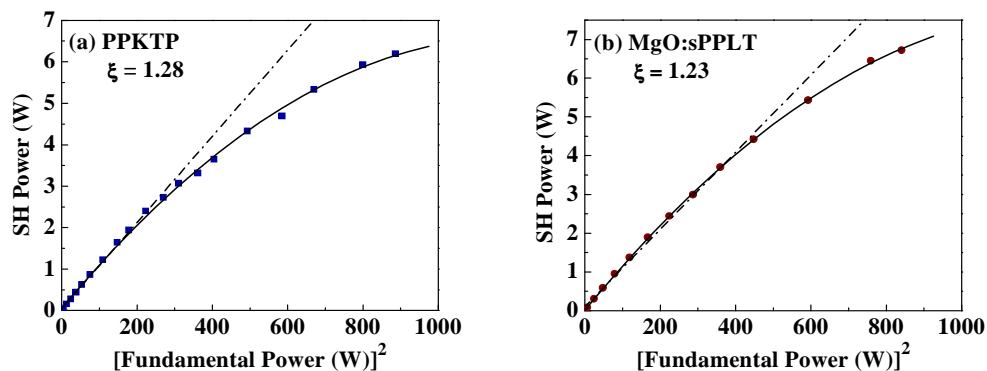


Fig. 6. Variation of the measured SH power with square of the fundamental power for (a) PPKTP, (b) MgO:sPPLT.

In MgO:sPPLT, we generated a maximum green power of 9.6 W at the fundamental power of 29.5 W with a beam waist radius of 31  $\mu\text{m}$  at the center of crystal, corresponding to a focusing parameter  $\xi=2.48$ . Similar attempts in PPKTP, however, led to increased SH output instabilities and power degradation with time at increased input intensities, as described in more detail in section 5.

In order to verify the contribution of thermal effects, we chopped the fundamental beam at a frequency of 530 Hz, with a 5.5% duty cycle, and performed power scaling measurements in both crystals by recording the dependence of the generated average SH power on the square of the average fundamental power. The results are shown in Fig. 7. As can be seen, the generated average SH power in both crystals follows a linear dependence on the average input power, confirming the contribution of thermal phase-mismatch effects to saturation under pure cw pumping. The linear variation is characterized by a slope-efficiency of 13.5 %/W in PPKTP and 14.6 %/W in MgO:sPPLT. The thermal dephasing effects can arise from linear and two-photon absorption at the fundamental and SH wavelengths and GRIIRA. To verify any contribution from GRIIRA to thermal dephasing, we focused 6 W of green radiation from a frequency-doubled cw Nd:YVO<sub>4</sub> laser at 532 nm (Coherent, Verdi-10) to a beam radius of 34  $\mu\text{m}$  inside the PPKTP crystal to obtain similar maximum green power density (0.33 MW/cm<sup>2</sup>) as in the SHG experiments. The arrangement resulted in the simultaneous focusing of the fundamental fiber laser beam to a waist radius of 28  $\mu\text{m}$  inside the PPKTP crystal, close to 37  $\mu\text{m}$  used in the SHG experiments. We then measured the variation in transmitted IR power at different green power levels over periods of ten minutes. However, we observed no difference in the transmitted IR power with and without green radiation, indicating the absence of

GRIIRA in PPKTP up to the maximum generated green power of 6 W. Earlier reports indicate no signature of GRIIRA in MgO:sPPLT at these power levels [19,20].

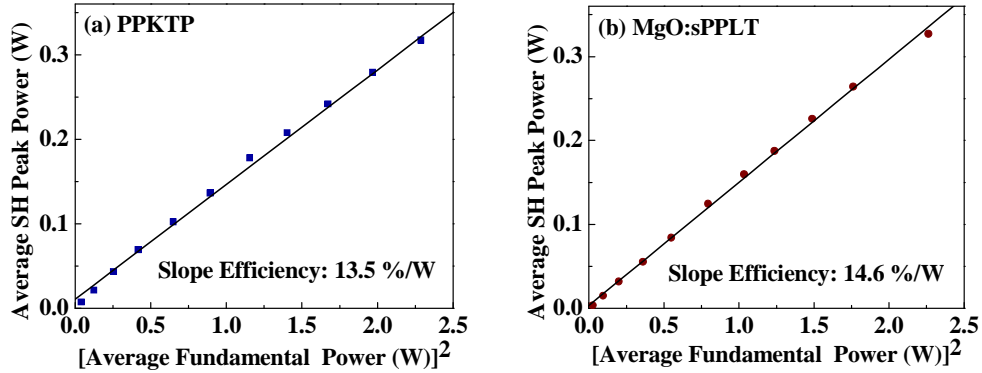


Fig. 7. Dependence of the measured average SH power on square of the average fundamental power for (a) PPKTP, (b) MgO:sPPLT.

We also investigated the possible role of TPA in PPKTP and MgO:sPPLT by recording the crystal transmission at both fundamental and green wavelengths at power levels up to 30 W and 6 W, respectively. The results for PPKTP are shown in Figs. 8 (a, b). We observed a linear increase in the transmitted power with input power at both wavelengths, from which linear absorption losses of 0.3%/cm at 1064 nm and 4.5%/cm at 532 nm were deduced. Figures 8(c, d) show similar measurements in MgO:sPPLT, resulting in a linear absorption loss of 0.17%/cm at 1064 nm and 1.57%/cm at 532 nm. These measurements thus confirm the role of intrinsic linear absorption at fundamental and SH wavelengths to thermal dephasing in both crystals, setting a limit to the maximum generated cw SH power [8, 10-12].

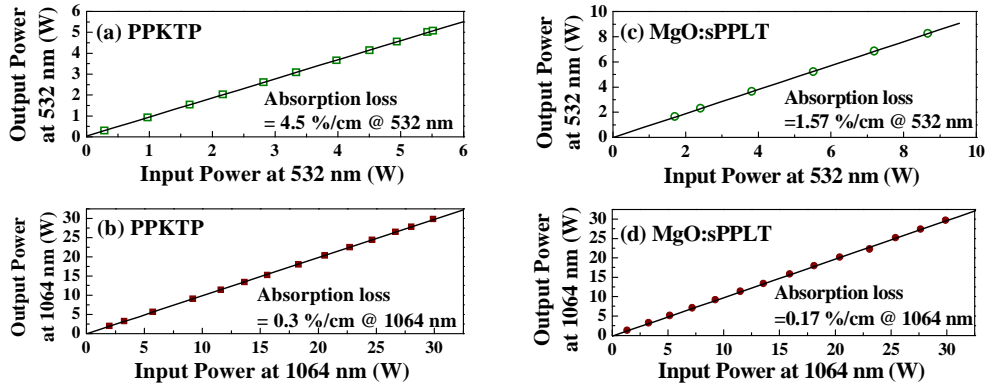


Fig. 8. Linear transmission of (a, b) PPKTP, and (c, d) MgO:sPPLT at fundamental and SH wavelengths.

We determined a normalized conversion efficiency of 1.2%/W for PPKTP and 1.3%/W for MgO:sPPLT in the low-power regime with a monotonous decrease in normalized efficiency at increased fundamental powers. The normalized efficiency of 1.2%/W and a focusing parameter of  $\xi=1.28$  result in a calculated effective nonlinearity of  $d_{eff}\sim 7.63$  pm/V, corresponding to  $d_{33}\sim 12$  pm/V for the 17 mm PPKTP crystal. For the 30 mm MgO:sPPLT sample, the 1.3%/W normalized efficiency and a focusing parameter of  $\xi=1.23$  result in a calculated  $d_{eff}\sim 7.00$  pm/V, corresponding to  $d_{33}\sim 11$  pm/V.

## 5. Power stability

In order to characterize the long-term stability of SHG output, we recorded the variation of the generated green power with time in both PPKTP and MgO:sPPLT crystals over a period of one hour. The measurements were performed at various fundamental power levels, focused to a fixed beam waist radius of 37  $\mu\text{m}$  in PPKTP and 44  $\mu\text{m}$  in MgO:sPPLT, at the center of the crystals. The results are shown in Fig. 9(a) for PPKTP and Fig. 9(b) for MgO:sPPLT. As evident in Fig. 9(a), in PPKTP the SH output power exhibits good stability with a peak-to-peak fluctuation ranging from 2.5% at 10 W to 8.6% at 20 W of input fundamental power. However, we observe degradation of SH power with time at higher fundamental powers approaching 25 W and above. We attribute this degradation to local heating of the PPKTP crystal due to absorption at the fundamental and SH wavelengths. After degradation of SH output power from an initial higher value to a lower value, changing the position of the focal spot by slightly translating the PPKTP crystal resulted in retaining the initially recorded high power, indicating that the light induced heating effect is highly localized in the region close to the path of the beam, which can be attributed to the relatively low thermal conductivity of PPKTP [6]. Previous measurements on cw SHG in PPKTP at fundamental powers up to 6.8 W and a phase-matching temperature of 148  $^{\circ}\text{C}$  have also revealed similar, but more severe, long-term degradation of SH power over a period of 15 hours [21]. Our results show the onset of SHG power degradation at substantially higher fundamental powers up to 25 W, which may be indicative of the superior quality of the PPKTP sample used in our experiment. The degradation of SH power in our measurements may be reduced by lowering the crystal temperature to compensate for thermal loading of the sample. However, due to the proximity of the optimum phase-matching to room temperature, Fig. 3(a), this would require cooling of the crystal, and as such could not be implemented with our present experimental setup.

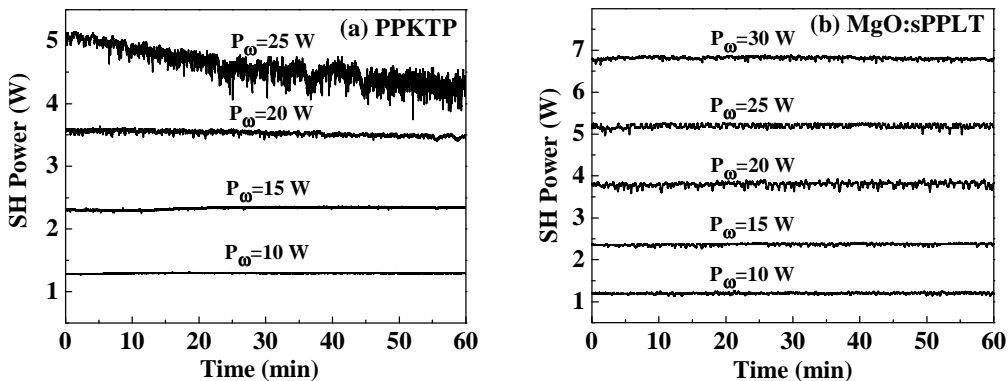


Fig. 9. Power stability recorded over one hour at various fundamental power levels for (a) PPKTP, and (b) MgO:sPPLT.

Similar measurements of SH output power stability in the MgO:sPPLT crystal are shown in Fig. 9(b). The peak-to-peak fluctuation in this case varies from 5.9% at 15 W to 3.5% at 29.5 W of fundamental power. Although the output power is observed to fluctuate about a mean value at the different fundamental power levels, which is mainly due to air currents in the laboratory, no noticeable degradation in SH power is observed with time, which can be attributed to the higher thermal conductivity of MgO:sPPLT [9]. In the absence of power degradation, we performed further long-term power reliability tests at higher fundamental powers. At the maximum available fundamental power of 29.5 W, we recorded a peak-to-peak power stability of 7.6% over 8 hours and 9% over 13 hours [11], confirming that MgO:sPPLT is a particularly promising material for high-power single-pass SHG into the green.

## 6. Further Optimization

The power scaling measurements under cw and quasi-cw conditions together with the crystal linear absorption loss measurements suggest the need for optimization and proper thermal management in order to improve the SHG efficiency. Considering the higher long-term power stability of SHG in the MgO:sPPLT crystal and the ability to withstand higher fundamental powers, further investigations were directed towards determination of the optimal focusing condition for the generation of maximum green power. Several different focusing conditions were deployed to achieve a fundamental beam waist radius ranging from 89  $\mu\text{m}$  down to 19  $\mu\text{m}$  at the center of the crystal, thereby varying the focusing parameter,  $\xi$ , from 0.32 to 6.6. Second harmonic power scaling measurements were then performed for each focusing condition up to the maximum available input fundamental power. The results are shown in Fig. 10, where the variation in single-pass SHG conversion efficiency and the corresponding phase-matching temperature are plotted for the different focusing parameters at a fundamental power of 29.5 W at the input to the crystal.

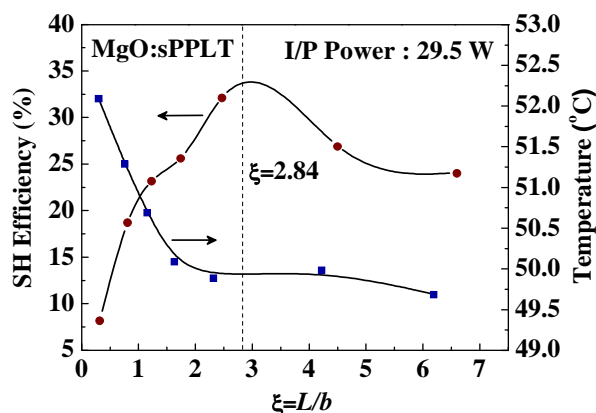


Fig. 10. SHG efficiency and corresponding phase-matching temperature as a function of focusing parameter,  $\xi=L/b$ , at a fundamental power of 29.5 W. The filled circles and squares are the experimental data and the solid lines are the best fit to the data. The vertical dashed line corresponds to the optimal focusing condition predicted by theory [18].

Interestingly, the extrapolated efficiency curve has a clear peak near  $\xi \sim 2.84$ , corresponding to the theoretical prediction of Boyd and Kleinman for optimum SHG in the cw (or long-pulse) limit [18]. It is clear from the data that for a fundamental beam waist radius between 23  $\mu\text{m}$  ( $\xi=4.50$ ) and 37  $\mu\text{m}$  ( $\xi=1.74$ ), single-pass SHG conversion efficiencies  $>25\%$  are available in the present experiment. We were able to use a near-optimum fundamental beam waist radius of 31  $\mu\text{m}$ , corresponding to a focusing parameter  $\xi=2.48$ , where we measured a SH power of 9.6 W at conversion efficiency of 32.7%, as shown in Fig. 11(a). However, the effect of saturation is still evident from the deviation of the linearity of SH power with the square of fundamental power as shown in Fig. 11(b). It is also evident from Fig. 10 that the SHG conversion efficiency rises sharply for increasing values of  $\xi$  from 0.32 to 2.48, while at the same time the phase-matching temperature decreases rapidly. On the other hand, with further increases in the value of  $\xi$  above 2.48, the SHG efficiency begins to drop, while the phase-matching temperature remains almost constant. There is a clear correlation between the rise in SHG conversion efficiency and the drop in the optimum phase-matching temperature.

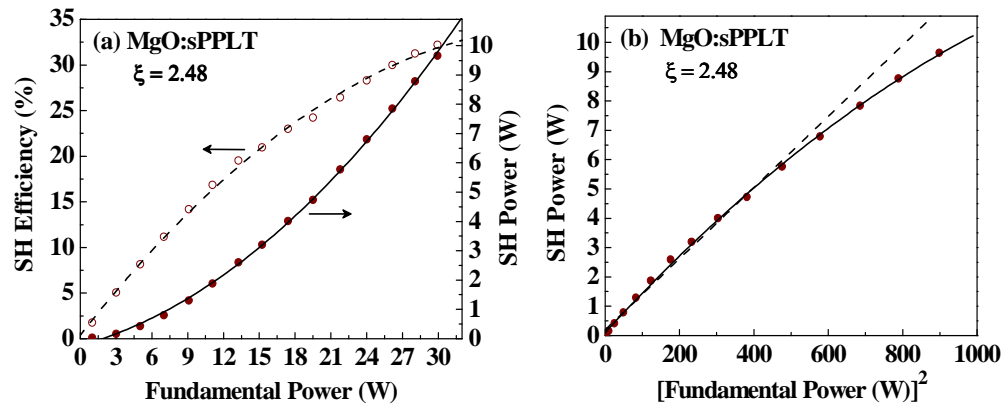


Fig. 11. Dependence of (a) measured SH power and corresponding conversion efficiency on the fundamental power and (b) measured SH power on the square of fundamental power.

Since the input pump power remains fixed, the contribution of linear absorption of fundamental to crystal heating and hence thermal effects remains the same for all the focusing conditions. Therefore, the major contribution to crystal heating is clearly from the absorption of the generated green power, which necessitates the reduction of the crystal temperature to achieve optimum phase-matching. However, given the significant linear absorption of 0.17%/cm at 1064 nm, the role of fundamental absorption to crystal heating can not be entirely neglected. To verify this contribution, under the focusing condition of  $\xi=1.74$ , we rotated the fundamental polarization such that the generated green power was less than 100 mW at 29.5 W of fundamental power. By increasing the fundamental power from 1 W to 29.5 W, we observed a drop in the PM temperature from 52.5°C to 51.6°C, clearly indicating still significant contribution of the fundamental absorption to thermal effects. These studies thus confirm that thermal effects in the MgO:sPPLT crystal were neither due to GRIIRA nor TPA, but a result of intrinsic linear absorption in the IR and green. We also investigated the variation in SHG efficiency with the focusing parameter,  $\xi$ , at various fundamental power levels, with the results shown in Fig. 12(a). Again, the dashed line corresponds to the optimum theoretical value of  $\xi \sim 2.84$  for maximum SHG efficiency [18], confirming near-optimum performance of our SHG setup at all fundamental power levels. We performed additional studies on the influence of focusing on phase-matching temperature over the full range of fundamental power levels. The result is shown in Fig. 12(b), where we clearly observe a shift in the phase-matching temperature to lower values with tighter focusing for all input fundamental powers, even at low input powers where thermal effects due to the absorption of the generated green and the fundamental are negligible. We believe this to be due to the increased angular divergence of the input fundamental beam with tighter focusing, which results in the propagation of the divergent components over longer grating periods. In MgO:sPPLT, this results in a shift in the phase-matching temperature for SHG to lower values. For example, at 1 W of input fundamental power, the optimum phase-matching temperature for SHG is reduced from 53 °C for  $\xi=0.32$  to 52.3 °C for  $\xi=6.6$ . This reduction of 0.7 °C corresponds to a difference in grating period of  $\Delta\Lambda=1.36$  nm, corresponding to the increased divergence of the pump beam when subjected to tighter focusing from  $w_0 \sim 89$   $\mu\text{m}$  down to  $w_0 \sim 19$   $\mu\text{m}$ . As a result, tighter focusing conditions result in an overall reduction in the optimum phase-matching temperature for SHG, even at low fundamental powers, where crystal heating effect due to thermal loading are negligible. A clear understanding of this phenomenon requires further theoretical analysis which is under investigation.

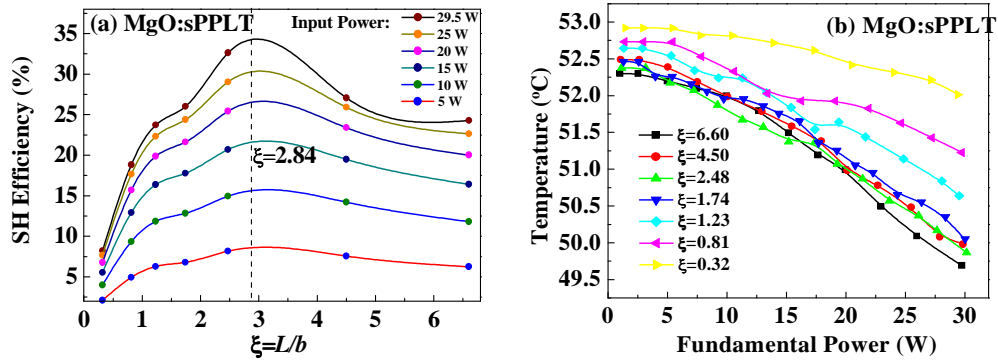


Fig. 12. (a) Dependence of SHG efficiency on focusing parameter,  $\xi=L/b$ , at various fundamental power levels and (b) variation of phase-matching temperature with fundamental power under different focusing conditions.

In order to further study the effects of crystal heating, due to light-induced linear absorption, on SHG conversion efficiency, we also investigated two different thermal management schemes based on different oven designs. In the first design (close-top), the oven encloses the crystal on all sides, except the input and output facets. In the second (open-top), the crystal is exposed to the ambient from the top as well as the input and output facets. We performed power scaling measurements using both designs under identical focusing conditions, using a fundamental optimum beam waist radius of  $31 \mu\text{m}$  ( $\xi=2.48$ ). The results are shown in Fig. 13. The data were collected by adjusting the phase-matching temperature for each fundamental power to obtain maximum SH green power. From the plot, we clearly observe a significant difference in the SHG efficiency using the two different oven designs, with the difference increasing at higher fundamental powers. The maximum SHG efficiency achieved at the full fundamental power using the close-top oven design is 26.43%, while the open-top oven configuration results in a maximum SH efficiency of 32.7%. We attribute this significant difference to the easier heat exchange between the crystal and the ambient air in the open-top oven design, which permits the required reduction in crystal temperature for optimum phase-matching to be achieved and maintained, whereas in the close-top design this optimum equilibrium condition is difficult to achieve. These observations imply that careful design of crystal heating components and the oven can also play an important role in the attainment of highest SHG efficiency. Increased SHG efficiency for 532 nm emission in periodically-poled near stoichiometric LiTaO<sub>3</sub> was demonstrated by compensating temperature non-uniformity along the beam propagation using two-zone temperature control [22]. So in our present work there may be scope for further improvements in generated green power with more stringent thermal management and control.

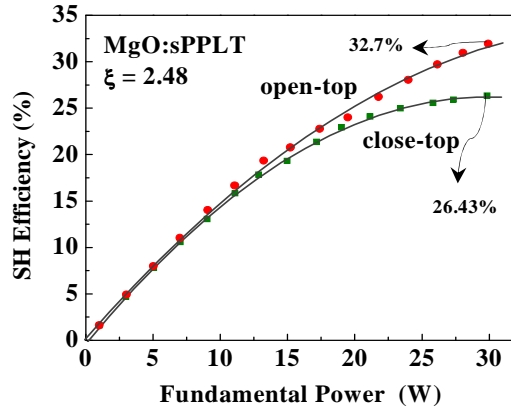


Fig. 13. SHG efficiency as a function of fundamental power in close-top and open-top crystal holder configurations.

### 7. Single-frequency operation and beam profile

We studied the spectral characteristics of the generated SH output in both PPKTP and MgO:sPPLT crystals to obtain information about the linewidth of the green radiation. Using a confocal scanning Fabry-Perot interferometer (free-spectral-range of 1 GHz; finesse of 400), we recorded the transmission fringes of the green output from both crystals at different fundamental power levels. In all cases, we obtained reliable single-frequency operation in

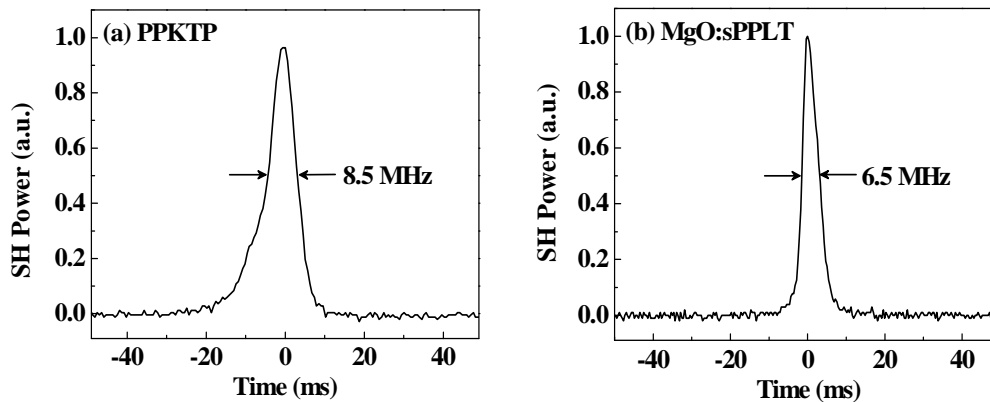


Fig. 14. Instantaneous linewidth of SHG in (a) PPKTP at 25 W of fundamental power, and (b) MgO:sPPLT at 30 W of fundamental power, measured with a scanning confocal Fabry-Perot interferometer.

both the crystals, which is not a surprising result, given the single-frequency nature of the input fundamental and its direct transfer to the SH output. To obtain instantaneous linewidth values, we recorded snap shots of the transmission fringe pattern through the interferometer and deduced the corresponding full-width at half-maximum (FWHM) bandwidths of the green from the measurements. Figure 14 shows typical transmission spectra at the maximum fundamental powers of 25 W for PPKTP and 30 W for MgO:sPPLT, corresponding to the maximum input power at which stable green output could be generated. The measurements resulted in an instantaneous SHG linewidth of 8.5 MHz in PPKTP and 6.5 MHz in MgO:sPPLT, limited by the resolution of the interferometer. For both crystals, we consistently obtained the same linewidth values at all fundamental powers. The larger linewidth measured

in PPKTP may be due to the shorter crystal length used, which would allow phase-matching over a larger range of fluctuations in the fundamental laser linewidth, than would be the case with the longer MgO:sPPLT sample with the correspondingly narrower spectral acceptance. We also investigated the frequency stability of the generated green radiation in MgO:sPPLT using a wavemeter (HighFinesse, WS-U 30). The measurements were performed at 9.6 W of green power, close to the maximum SHG efficiency, under free-running conditions, and in the absence of any thermal isolation. The results are shown in Fig. 15, where it can be seen that the green output exhibits a passive frequency stability with a peak-to-peak fluctuation of <115 MHz over 90 minutes. Further, a short-term stability of <32 MHz over 30 minutes and a long-term stability of <370 MHz over 12 hours have been recorded for SHG from MgO:sPPLT.

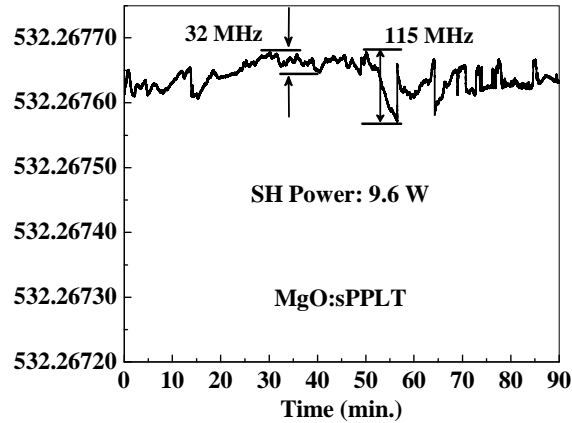


Fig. 15. Frequency stability of MgO:sPPLT recorded over 90 minutes at 9.6 W of SH power.

The far-field energy distribution of the SHG is determined by recording the spatial beam profile at different fundamental power levels. Fig. 16 shows the beam profile at a fundamental power of 25 W in both the crystals. Although the beam profile of SHG from PPKTP remained symmetric in the low power regime, the beam is found to be distorted in the high power regime. However, the SHG output beam from MgO:sPPLT remained symmetric even at the maximum fundamental power of 29.5 W.

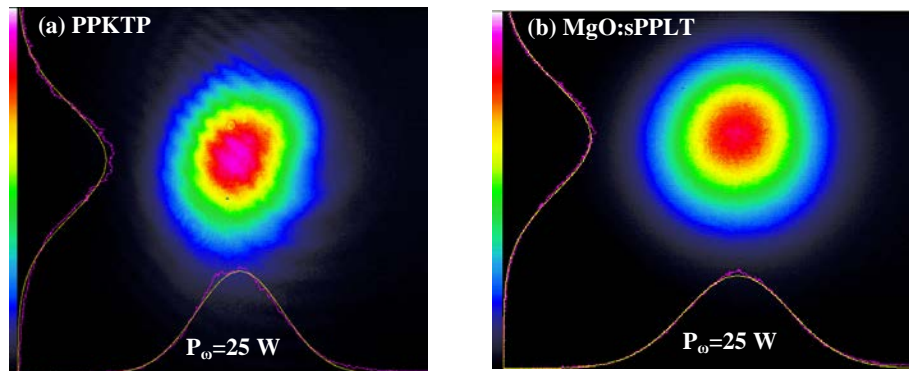


Fig. 16. Second harmonic beam profile at a fundamental power of 25 W generated in (a) PPKTP, and (b) MgO:sPPLT.

Figure 17 shows the variation of  $M^2$  value of the generated green beam measured by scanning a beam profiler across the Rayleigh range of the focused beam. The measurements were performed using a fundamental beam waist radius of  $37\ \mu\text{m}$ , corresponding to a focusing parameter  $\xi=1.74$  in MgO:sPPLT and  $\xi=1.28$  in PPKTP. A slight variation of  $M_x^2$  from 1.25 to 1.29 and  $M_y^2$  from 1.2 to 1.34 is recorded for SHG in PPKTP. Similar measurements for MgO:sPPLT resulted in  $M_x^2$  varying from 1.11 to 1.29 and  $M_y^2$  from 1.17 to 1.33, at different input power levels.

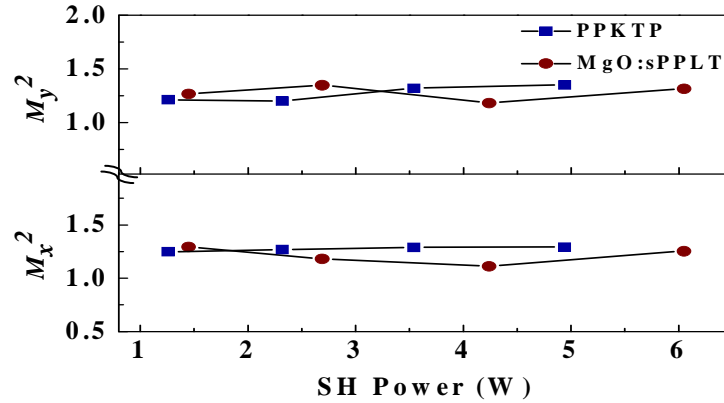


Fig. 17. Beam quality  $M^2$  values of generated green radiation measured as a function of SH power.

## 8. Conclusions

In conclusion, we have presented detailed studies on the generation of watt-level, cw, single-frequency radiation at 532 nm using a simple single-pass SHG of an ytterbium fiber laser in periodically poled nonlinear crystals of PPKTP and MgO:sPPLT. We have demonstrated a maximum SH green power of 9.6 W at a single-pass efficiency of 32.7% in MgO:sPPLT and 6.2 W at a conversion efficiency of 20.8% in PPKTP. Single-pass SHG characteristics of PPKTP and MgO:sPPLT have been studied and compared. Thermal effects have been confirmed by quasi-cw power scaling and cw linear absorption measurements. Further optimization in MgO:sPPLT revealed that maximum SH power and conversion efficiency can be obtained by deploying optimal focusing conditions and thermal isolation using suitable oven design. Power stability measurements performed in both crystals revealed a peak-to-peak power fluctuation of 8.6% over 1 hour at fundamental power of 20 W in PPKTP, while in MgO:sPPLT a long-term power stability with a peak-to-peak fluctuation of 9% was recorded over 13 hours at a fundamental power of 29.5 W, confirming that stable and high-power generation with negligible power degradation is possible with MgO:sPPLT. The generated green radiation exhibited an instantaneous linewidth of 8.5 MHz in PPKTP and 6.5 MHz in MgO:sPPLT, with the green output from MgO:sPPLT exhibiting a frequency stability of <115 MHz over 90 minutes, a short-term stability of <32 MHz over 30 minutes, and a long-term stability of <370 MHz over 12 hours. Spatial beam profiles with  $M^2 < 1.34$  and  $M^2 < 1.33$  were measured for the generated green beam in PPKTP and MgO:sPPLT, respectively. The beam quality of SHG in PPKTP was found to be distorted at fundamental power >20 W, while it remained intact with circularity >96% and no noticeable distortion up to a fundamental power of 29.5 W for SHG in MgO:sPPLT. Further improvements in SH efficiency and power stability are expected with improved thermal management of crystal heating effects, opening up the possibility of power scaling the green output with increased fundamental powers and longer crystal interaction lengths.

## **Acknowledgments**

The authors thank C. Canalias, V. Pasiskevicius, and F. Laurell of the Royal Institute of Technology, Sweden, for providing the PPKTP crystal. This research was supported by the Ministry of Education and Science, Spain, through grants TEC2006-12360 and the Consolider project, SAUUL (CSD2007-00013). We also acknowledge partial support of this research by the Seventh Framework Program of the European Union - MIRSURG (224042).